

QCD corrections to J/ψ production in association with a W -boson at the LHC

Li Gang^(a), Song Mao^(b), Zhang Ren-You^(b), and Ma Wen-Gan^(b)

^(a) School of Physics and Material Science, Anhui University, Hefei, Anhui 230039, P.R.China

^(b) Department of Modern Physics, University of Science and Technology of China (USTC),
Hefei, Anhui 230026, P.R.China

We calculate the next-to-leading order (NLO) QCD corrections to the $J/\psi + W$ production at the LHC, and provide the theoretical distribution of the J/ψ transverse momentum. Our results show that the differential cross section $\frac{d\sigma}{dp_T^{J/\psi}}$ at the LO is significantly enhanced by the NLO QCD corrections. We believe that the comparison between the theoretical predictions for the $J/\psi + W$ production and the experimental data at the LHC can provide a verification for the colour-octet mechanism of non-relativistic QCD in the description of the processes involving heavy quarkonium.

PACS numbers: 12.38.Bx, 12.39.St, 13.60.Le

The study of heavy quarkonium is one of the most interesting subjects in both theoretical and experimental physics, which offers a good ground for investigating Quantum Chromodynamics (QCD) in both perturbative and non-perturbative regimes. The factorization formalism of nonrelativistic QCD (NRQCD) [1] provides a rigorous theoretical framework to describe the heavy-quarkonium production and decay by separating the transition rate (production cross section or decay rate) into two parts, the short-distance part which can be expanded as a power series in α_s and calculated perturbatively, and the long-distance matrix elements (LDMEs) which can be extracted from experiments. The importance of the LDMEs can be estimated by using velocity scaling rules [2]. A crucial feature of the NRQCD is that the complete structure of the quarkonium Fock space has been explicitly considered.

By introducing the color-octet mechanism (COM), the NRQCD has successfully absorbed the infrared divergences in P-wave [1, 3, 4] and D-wave [5, 6] decay widths of heavy quarkonium, which can not be handled in the color-singlet mechanism (CSM). The COM can successfully reconcile the orders of magnitude of the discrepancies between the experimental data of J/ψ production at the Tevatron [7] and the CSM theoretical predictions, even if they have been calculated up to the NLO. The DELPHI data also favor the NRQCD COM predictions for the $\gamma\gamma \rightarrow J/\psi + X$ process [8, 9]. Similarly the recent experimental data on the J/ψ photo-production of H1 [10] are fairly well described by the complete NLO NRQCD corrections [11], and give a strong support to the existence of the COM. However, the observed cross sections for the double charmonium production at B factories [12] are much larger than the LO NRQCD prediction [13]. This discrepancy can be resolved by considering the CSM NLO QCD correc-

tions [14] and the relativistic corrections [15] without invoking the color-octet contributions [16]. Furthermore, the J/ψ polarization in hadroproduction at the Tevatron [17] and photo-production at the HERA [18] also conflict with the NRQCD predictions. Therefore, the existence of the COM is still under doubt and far from being proven. The further tests for the CSM and COM under the NRQCD in heavy quarkonium production are still needed.

In order to test the COM, it is an urgent task to study the processes which significantly depend on the production mechanism. The J/ψ production associated with a W boson at the LHC, $pp \rightarrow J/\psi + W + X$, can serve as a such kind of process [19]. For this process, only the 3S_1 color-octet (the $c\bar{c}[^3S_1^{(8)}]$ Fock state) provides contribution at the leading-order (LO). Even including the NLO QCD corrections up to the $\alpha_s^3 v^7$ order, there are only color-octets $c\bar{c}[^1S_0^{(8)}]$, $c\bar{c}[^3S_1^{(8)}]$ and $c\bar{c}[^3P_J^{(8)}]$ ($J = 0, 1, 2$), but no color-singlet contribution exists in the $pp \rightarrow J/\psi + W + X$ process. Therefore, the $J/\psi + W$ production at the LHC is an ideal ground to study the COM.

As we know, the NLO QCD corrections to quarkonium production are usually significant [14, 20, 21]. We should generally take the NLO QCD corrections into account in studying the COM and the universality of the LDMEs. In this paper, we calculate the $J/\psi + W$ production at the LHC up to the $\alpha_s^3 v^7$ order within the NRQCD framework by applying the covariant projection method [4], and present the theoretical prediction of the $p_T^{J/\psi}$ distribution. The LO cross section for the parent process $pp \rightarrow J/\psi + W^\pm + X$ involves the contributions of the following partonic processes,

$$u\bar{d} \rightarrow c\bar{c}[^3S_1^{(8)}] + W^+, \quad d\bar{u} \rightarrow c\bar{c}[^3S_1^{(8)}] + W^-. \quad (1)$$

Since the cross sections for the $u\bar{d} \rightarrow c\bar{c}[^3S_1^{(8)}] + W^+$

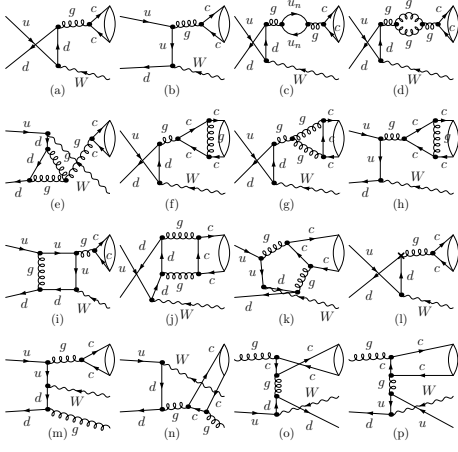


FIG. 1: Representative Feynman diagrams for $pp \rightarrow J/\psi + W^+$.

and $d\bar{u} \rightarrow c\bar{c}[^3S_1^{(8)}] + W^-$ partonic processes are the same due to the CP-conservation, we present only the detailed description for the calculation of the partonic process $u(p_1)\bar{d}(p_2) \rightarrow c\bar{c}[^3S_1^{(8)}](p_3) + W^+(p_4)$. The tree-level diagrams for this partonic process are drawn in Figs.1(a)-(b).

In the nonrelativistic limit, by applying the covariant projection method [4] we obtain the differential cross section for $u\bar{d} \rightarrow c\bar{c}[^3S_1^{(8)}] + W^+$ expressed as

$$\frac{d\hat{\sigma}_0}{d\hat{t}} = \frac{\langle O^{J/\psi}[^3S_1^{(8)}] \rangle}{16\pi\hat{s}^2 N_{col}(^3S_1^{(8)}) N_{pol}(^3S_1^{(8)})} \frac{64g^2\alpha_s^2\pi^2}{9m_{J/\psi}^3\hat{t}^2\hat{u}^2} \times \left\{ -m_w^2 m_{J/\psi}^2 (\hat{t}^2 + \hat{u}^2) + \hat{t}\hat{u} [2\hat{s}^2 + \hat{t}^2 + \hat{u}^2 + 2\hat{s}(\hat{t} + \hat{u})] \right\}, \quad (2)$$

where $\hat{s} = (p_1 + p_2)^2$, $\hat{t} = (p_1 - p_3)^2$ and $\hat{u} = (p_1 - p_4)^2$. $N_{col}(^3S_1^{(8)})$ and $N_{pol}(^3S_1^{(8)})$ refer to the color and polarization degrees of freedom of $c\bar{c}[^3S_1^{(8)}]$ [4], respectively. Then the LO cross section for the $pp \rightarrow J/\psi + W^+ + X$ process is

$$\sigma^{(0)} = \int dx_1 dx_2 d\hat{\sigma}_0 [G_{u/A}(x_1, \mu_f) G_{\bar{d}/B}(x_2, \mu_f) + (A \leftrightarrow B)], \quad (\hat{s} = x_1 x_2 s), \quad (3)$$

where $G_{u,\bar{d}/A,B}$ are the parton distribution functions (PDFs), and A, B represent the two incoming protons at the LHC.

In calculating the NLO QCD corrections to the $pp \rightarrow J/\psi + W^+ + X$ process, we should consider both the virtual correction and the real gluon/light-quark emission correction. The virtual corrections only come from the $c\bar{c}[^3S_1^{(8)}]$ Fock state, while the real gluon/light-quark emission correction involves the

contributions of the $c\bar{c}[^1S_0^{(8)}]$, $c\bar{c}[^3S_1^{(8)}]$ and $c\bar{c}[^3P_J^{(8)}]$ ($J = 0, 1, 2$) Fock states. In our calculations, we adopt the dimensional regularization (DR) scheme to regularize the UV and IR divergences, and the modified minimal subtraction ($\overline{\text{MS}}$) and on-mass-shell schemes to renormalize the strong coupling constant and the quark wave functions, respectively.

There are 41 virtual QCD one-loop diagrams for the subprocess $u\bar{d} \rightarrow J/\psi + W^+$, which include self-energy (12), vertex (10), box (7), pentagon (2) and counterterm (10) diagrams. We present part of these diagrams in Figs.1(c)-(l). There exist ultraviolet (UV), Coulomb and soft/collinear infrared (IR) singularities in the virtual correction. The UV singularities are canceled by the counterterms of the strong coupling constant and the quark wave functions after the renormalization procedure. But the QCD one-loop amplitude of the partonic process $u\bar{d} \rightarrow c\bar{c}[^3S_1^{(8)}] + W^+$ still contains Coulomb and soft/collinear IR singularities. The IR and Coulomb singularities in the virtual correction can be expressed as

$$d\hat{\sigma}^V = d\hat{\sigma}_0 \left[\frac{\alpha_s}{2\pi} \frac{\Gamma(1-\epsilon)}{\Gamma(1-2\epsilon)} \left(\frac{4\pi\mu_r^2}{\hat{s}} \right)^\epsilon \right] \left(\frac{A_2^V}{\epsilon^2} + \frac{A_1^V}{\epsilon} - \frac{\pi^2}{6\nu} + A_0^V \right), \quad (4)$$

where

$$A_2^V = -2C_F, \quad A_1^V = -7 + 3 \left(\ln \frac{4m_c^2 - \hat{t}}{m_c \sqrt{\hat{s}}} + \ln \frac{4m_c^2 - \hat{u}}{m_c \sqrt{\hat{s}}} \right), \quad C_F = 4/3. \quad (5)$$

The soft/collinear IR singularities can be canceled by adding the contributions of the real gluon and light-quark emission partonic processes, and redefining the parton distribution functions at the NLO. For the Coulomb singularities, they can be canceled after taking into account the corresponding corrections to the operator $\langle O^{J/\psi}[^3S_1^{(8)}] \rangle$. We use the expressions in Refs.[22–24] to implement the numerical evaluations of IR-safe one-point, 2-point, 3-point, 4-point and 5-point integrals. In our calculations, only two diagrams, Figs.1(f) and (h), contain the Coulomb singularities, which are regularized by a small relative velocity ν between c and \bar{c} [25]. We adopt the expressions in Ref.[26] to deal with the IR-divergent Feynman integral functions.

The real gluon emission process provides three types of corrections, which correspond to the contributions from the $c\bar{c}[^1S_0^{(8)}]$, $c\bar{c}[^3S_1^{(8)}]$ and $c\bar{c}[^3P_J^{(8)}]$ ($J = 0, 1, 2$) Fock states, respectively. The real gluon emission correction to the $u\bar{d} \rightarrow c\bar{c}[^1S_0^{(8)}] + W^+$ subprocess is free of divergence, and can be numerically calculated by using

the Monte Carlo method. For the $c\bar{c}[^3S_1^{(8)}] + W^+ + g$ production, it contains both soft and collinear IR singularities which can be conveniently isolated by adopting the two cutoff phase space slicing (TCPSS) method [27].

In adopting the TCPSS method, we should introduce two arbitrary cutoffs, δ_s and δ_c . The phase space of the $u\bar{d} \rightarrow c\bar{c}[^3S_1^{(8)}] + W^+ + g$ subprocess can be split up into two regions, $E_5 \leq \delta_s \sqrt{\hat{s}}/2$ (soft gluon region) and $E_5 > \delta_s \sqrt{\hat{s}}/2$ (hard gluon region) by soft cutoff δ_s . Furthermore, the hard gluon region is separated as hard collinear (HC) and hard non-collinear ($\overline{\text{HC}}$) regions. The HC region is the phase space where $-\hat{t}_{15}$ (or $-\hat{t}_{25}$) $< \delta_c \hat{s}$ ($\hat{t}_{15} \equiv (p_1 - p_5)^2$ and $\hat{t}_{25} \equiv (p_2 - p_5)^2$). Therefore, the cross section for the real gluon emission subprocess can be expressed as

$$\begin{aligned}\hat{\sigma}_g^R(^3S_1^{(8)}) &= \hat{\sigma}_g^S(^3S_1^{(8)}) + \hat{\sigma}_g^H(^3S_1^{(8)}) \\ &= \hat{\sigma}_g^S(^3S_1^{(8)}) + \hat{\sigma}_g^{\text{HC}}(^3S_1^{(8)}) + \hat{\sigma}_g^{\overline{\text{HC}}}(^3S_1^{(8)}).\end{aligned}\quad (6)$$

The cross section for the subprocess $u\bar{d} \rightarrow c\bar{c}[^3S_1^{(8)}] + W^+ + g$ in the hard non-collinear ($\overline{\text{HC}}$) region is free of divergence, and can be numerically calculated by using the Monte Carlo method. The differential cross section for the subprocess $u\bar{d} \rightarrow c\bar{c}[^3S_1^{(8)}] + W^+ + g$ in the soft region can be expressed as

$$\begin{aligned}d\hat{\sigma}_g^S(^3S_1^{(8)}) &= -\frac{\alpha_s}{2\pi} \left\{ \frac{1}{6} [g(p_1, p_2) + g(p_c, p_{\bar{c}})] \right. \\ &\quad \left. - \frac{7}{6} [g(p_1, p_c) + g(p_2, p_{\bar{c}})] - \frac{1}{3} [g(p_1, p_{\bar{c}}) \right. \\ &\quad \left. + g(p_2, p_c)] \right\} d\hat{\sigma}_0,\end{aligned}\quad (7)$$

where $g(p_i, p_j)$ are soft integral functions defined as [28–30]

$$\begin{aligned}g(p_i, p_j) &= \frac{(2\pi\mu_r)^{2\epsilon}}{2\pi} \int_{E_5 \leq \delta_s \sqrt{\hat{s}}/2} \frac{d^{D-1}p_5}{E_5} \left[\frac{2(p_i \cdot p_j)}{(p_i \cdot p_5)(p_j \cdot p_5)} \right. \\ &\quad \left. - \frac{p_i^2}{(p_i \cdot p_5)^2} - \frac{p_j^2}{(p_j \cdot p_5)^2} \right].\end{aligned}$$

Then we can get

$$\begin{aligned}d\hat{\sigma}_g^S(^3S_1^{(8)}) &= d\hat{\sigma}_0 \left[\frac{\alpha_s}{2\pi} \frac{\Gamma(1-\epsilon)}{\Gamma(1-2\epsilon)} \left(\frac{4\pi\mu_r^2}{\hat{s}} \right)^\epsilon \right] \times \\ &\quad \times \left(\frac{A_2^S}{\epsilon^2} + \frac{A_1^S}{\epsilon} + A_0^S \right),\end{aligned}\quad (9)$$

where

$$A_2^S = 2C_F, \quad A_1^S = 3 - 3 \left(\ln \frac{4m_c^2 - \hat{t}}{m_c \sqrt{\hat{s}}} + \ln \frac{4m_c^2 - \hat{u}}{m_c \sqrt{\hat{s}}} \right).\quad (10)$$

For the subprocess $u\bar{d} \rightarrow c\bar{c}[^3S_1^{(8)}] + W^+ + g$ only the gluon radiation from initial particles can induce collinear singularities. The differential cross section, $d\hat{\sigma}_g^{\text{HC}}$, can be written as

$$\begin{aligned}d\sigma_g^{\text{HC}} &= d\hat{\sigma}_0 \left[\frac{\alpha_s}{2\pi} \frac{\Gamma(1-\epsilon)}{\Gamma(1-2\epsilon)} \left(\frac{4\pi\mu_r^2}{\hat{s}} \right)^\epsilon \right] \left(-\frac{1}{\epsilon} \right) \times \\ &\quad \times \delta_c^{-\epsilon} \left[P_{uu}(z, \epsilon) G_{u/A}(x_1/z, \mu_f) G_{\bar{d}/B}(x_2, \mu_f) + \right. \\ &\quad \times P_{\bar{d}\bar{d}}(z, \epsilon) G_{\bar{d}/B}(x_2/z, \mu_f) G_{u/A}(x_1, \mu_f) + (A \leftrightarrow B) \Big] \\ &\quad \times \frac{dz}{z} \left(\frac{1-z}{z} \right)^{-\epsilon} dx_1 dx_2,\end{aligned}\quad (11)$$

where $P_{uu}(z, \epsilon)$ and $P_{\bar{d}\bar{d}}(z, \epsilon)$ are the D-dimensional unregulated ($z < 1$) splitting functions related to the usual Altarelli-Parisi splitting kernels [31]. $P_{ii}(z, \epsilon)$ ($i = u, \bar{d}$) can be written explicitly as

$$\begin{aligned}P_{ii}(z, \epsilon) &= P_{ii}(z) + \epsilon P'_{ii}(z) \\ P_{ii}(z) &= C_F \frac{1+z^2}{1-z} \\ P'_{ii}(z) &= -C_F(1-z) \quad (i = u, \bar{d}).\end{aligned}\quad (12)$$

As for the partonic process $u\bar{d} \rightarrow c\bar{c}[^3P_J^{(8)}] + W^+ + g$, it contains only the soft singularities. Using the TCPSS method mentioned above, we split the phase space up into soft gluon region and hard gluon region by adopting the cutoff δ_s . Then the cross section for the partonic process $u\bar{d} \rightarrow c\bar{c}[^3P_J^{(8)}] + W^+ + g$ can be expressed as

$$\hat{\sigma}_g^R(^3P_J^{(8)}) = \hat{\sigma}_g^S(^3P_J^{(8)}) + \hat{\sigma}_g^H(^3P_J^{(8)}).\quad (13)$$

The cross section $\hat{\sigma}_g^H(^3P_J^{(8)})$ is finite and can be evaluated in four dimensions by using Monte Carlo method. The differential cross section in the soft region for the process $u\bar{d} \rightarrow c\bar{c}[^3P_J^{(8)}] + W^+ + g$, $d\hat{\sigma}_g^S(^3P_J^{(8)})$, can be expressed as

$$\begin{aligned}(8) \quad d\hat{\sigma}_g^S(^3P_J^{(8)}) &= -\left(\frac{1}{\epsilon} - 2\ln\delta_s + \frac{1}{\beta} \ln \frac{1+\beta}{1-\beta} \right) \frac{4\alpha_s B_F}{3\pi m_c^2} \\ &\quad \times \frac{\Gamma(1-\epsilon)}{\Gamma(1-2\epsilon)} \left(\frac{4\pi\mu_r^2}{\hat{s}} \right)^\epsilon < O^{J/\psi} [^3P_J^{(8)}] > \\ &\quad \times \frac{d\hat{\sigma}_0}{< O^{J/\psi} [^3S_1^{(8)}] >}\end{aligned}\quad (14)$$

with $\beta = \sqrt{1 - 4m_c^2/E_3^2}$ and $E_3 = \frac{\hat{s} + 4m_c^2 - m_w^2}{2\sqrt{\hat{s}}}$.

The real light-quark corrections to the subprocess $u\bar{d} \rightarrow J/\psi + W^+$ arise from the partonic processes

$$g(p_1)u(\bar{d})(p_2) \rightarrow c\bar{c}[n](p_3) + W^+(p_4) + d(\bar{u})(p_5),\quad (15)$$

where $n = {}^3S_1^{(8)}, {}^1S_0^{(8)}$ and ${}^3P_J^{(8)}$. Some of the Feynman diagrams for these partonic processes are presented in Figs.1(o)-(p).

The real light-quark partonic processes with $n = {}^1S_0^{(8)}$ and ${}^3P_J^{(8)}$ contain no singularities, so we can perform their phase space integrations by using the general Monte Carlo method. The partonic processes $gu(\vec{d}) \rightarrow c\bar{c}[{}^3S_1^{(8)}] + W^+ + d(\vec{u})$ contain only the initial state collinear singularities. By using the TCPSS method, we split the phase space up into two regions, collinear region and non-collinear region,

$$\hat{\sigma}_q^R({}^3S_1^{(8)}) = \hat{\sigma}_q^C({}^3S_1^{(8)}) + \hat{\sigma}_q^{\bar{C}}({}^3S_1^{(8)}) \quad (q = u, \vec{d}). \quad (16)$$

The cross section in non-collinear region, $\hat{\sigma}_q^{\bar{C}}({}^3S_1^{(8)})$ is finite and can be evaluated in four dimensions by using the Monte Carlo method. The differential cross sections for the subprocesses $gu(\vec{d}) \rightarrow c\bar{c}({}^3S_1^{(8)}) + W^+ + d(\vec{u})$ can be written as

$$\begin{aligned} d\sigma_q^C({}^3S_1^{(8)}) &= d\hat{\sigma}_0 \left[\frac{\alpha_s}{2\pi} \frac{\Gamma(1-\epsilon)}{\Gamma(1-2\epsilon)} \left(\frac{4\pi\mu_r^2}{\hat{s}} \right)^\epsilon \right] \left(-\frac{1}{\epsilon} \right) \\ &\times \delta_c^{-\epsilon} [P_{\vec{d}(u)g}(z, \epsilon) G_{g/A}(x_1/z, \mu_f) G_{u(\vec{d})/B}(x_2, \mu_f) \\ &+ (A \leftrightarrow B)] \frac{dz}{z} \left(\frac{1-z}{z} \right)^{-\epsilon} dx_1 dx_2 \end{aligned} \quad (17)$$

with $q = u, \vec{d}$ and $P_{qg}(z, \epsilon)$ can be expressed explicitly as

$$\begin{aligned} P_{qg}(z, \epsilon) &= P_{qg}(z) + \epsilon P'_{qg}(z), \\ P_{qg}(z) &= \frac{1}{2} [z^2 + (1-z)^2], \\ P'_{qg}(z) &= -z(1-z). \end{aligned} \quad (18)$$

To obtain an IR-safe cross section for the $pp \rightarrow J/\psi + W^+ + X$ up to the NLO, we should take into account both the NLO QCD counterterms of the PDFs and the NLO QCD corrections to the operator $\langle \mathcal{O}^{J/\psi}[{}^3S_1^{(8)}] \rangle$. The $\mathcal{O}(\alpha_s)$ counterterms of the PDFs are expressed as [32]

$$\begin{aligned} \delta G_{i/A}(x, \mu_f) &= \frac{1}{\epsilon} \left[\frac{\alpha_s}{2\pi} \frac{\Gamma(1-\epsilon)}{\Gamma(1-2\epsilon)} \left(\frac{4\pi\mu_r^2}{\mu_f^2} \right)^\epsilon \right] \\ &\times \int_z^1 \frac{dz}{z} P_{ij}(z) G_{j/A}(x/z, \mu_f). \end{aligned} \quad (19)$$

By adding the contributions of the PDF counterterms and the real gluon/light-quark emission collinear corrections shown in Eqs.(11) and (17), we obtain

$$d\sigma^{coll} = d\hat{\sigma}_0 \left[\frac{\alpha_s}{2\pi} \frac{\Gamma(1-\epsilon)}{\Gamma(1-2\epsilon)} \left(\frac{4\pi\mu_r^2}{\hat{s}} \right)^\epsilon \right] \{ \tilde{G}_{u/A}(x_1, \mu_f)$$

$$\begin{aligned} &\times G_{\vec{d}/B}(x_2, \mu_f) + G_{u/A}(x_1, \mu_f) \tilde{G}_{\vec{d}/B}(x_2, \mu_f) \\ &+ \sum_{\alpha=u, \vec{d}} \left[\frac{A_1^{sc}(\alpha \rightarrow \alpha g)}{\epsilon} + A_0^{sc}(\alpha \rightarrow \alpha g) \right] G_{u/A}(x_1, \mu_f) \\ &\times G_{\vec{d}/B}(x_2, \mu_f) + (A \leftrightarrow B) \} dx_1 dx_2, \end{aligned} \quad (20)$$

where

$$\begin{aligned} A_1^{sc}(\alpha \rightarrow \alpha g) &= C_F(2 \ln \delta_s + 3/2), \\ A_0^{sc} &= A_1^{sc} \ln \left(\frac{\hat{s}}{\mu_f^2} \right), \quad \alpha = u, \vec{d} \end{aligned} \quad (21)$$

and

$$\begin{aligned} \tilde{G}_{\alpha/H}(x, \mu_f) &= \sum_{\alpha'=\alpha, g} \int_x^{1-\delta_s \delta_{\alpha\alpha'}} \frac{dy}{y} G_{\alpha'/H}(x/y, \mu_f) \tilde{P}_{\alpha\alpha'}(y), \\ (H &= A, B, \alpha = u, \vec{d}), \end{aligned} \quad (22)$$

with

$$\tilde{P}_{\alpha\alpha'}(y) = P_{\alpha\alpha'} \ln \left(\delta_c \frac{1-y}{y} \frac{\hat{s}}{\mu_f^2} \right) - P'_{\alpha\alpha'}(y). \quad (23)$$

We can see that the summation of the soft (Eq.(9)), collinear (Eq.(20)), and UV renormalized virtual corrections (Eq.(4)) to the $pp \rightarrow J/\psi + W^+ + X$ process, $d\sigma_g^S + d\sigma^{coll} + d\sigma^V$, is soft/collinear IR- and UV-finite, i.e.,

$$\begin{aligned} A_2^S + A_2^V &= 0, \\ A_1^S + A_1^V + A_1^{sc}(u \rightarrow ug) + A_1^{sc}(\vec{d} \rightarrow \vec{d}g) &= 0. \end{aligned} \quad (24)$$

However the above result, $d\sigma_g^S + d\sigma^{coll} + d\sigma^V$, still contains the Coulomb singularity. Furthermore, the corrections contributed by the $c\bar{c}[{}^3P_J^{(8)}]$ ($J = 0, 1, 2$) Fock states, $d\hat{\sigma}_g^R({}^3P_J^{(8)})$, contain soft IR singularities too. We can eliminate these singularities by taking into account the NLO QCD corrections to the operator $\langle \mathcal{O}^{J/\psi}[{}^3S_1^{(8)}] \rangle$. In this paper we use the method in Ref.[4] to deal with these singularities. In Fig.2 we present the IR and Coulomb singularities structure in the NLO QCD calculations for the $pp \rightarrow J/\psi + W^+ + X$ process. We have checked analytically that all the IR and Coulomb singularities are canceled in the final result.

The final result for the process $pp \rightarrow J/\psi + W^+ + X$ up to the NLO consists of three parts of contributions,

$$\sigma_{total} = \sigma_{{}^3S_1^{(8)}} + \sigma_{{}^1S_0^{(8)}} + \sigma_{{}^3P_J^{(8)}}, \quad (25)$$

where $\sigma_{{}^3S_1^{(8)}}$ can be divided into two parts: a two-body term $\sigma_{{}^3S_1^{(8)}}^{(2)}$ and a three-body term $\sigma_{{}^3S_1^{(8)}}^{(3)}$. The two-body

term, $\sigma_{3S_1^{(8)}}^{(2)}$, is expressed as

$$\begin{aligned} \sigma_{3S_1^{(8)}}^{(2)} = & \sigma^{(0)} + \frac{\alpha_s}{2\pi} \int dx_1 dx_2 d\hat{\sigma}_0 \{ G_{u/A}(x_1, \mu_f) \\ & \times G_{\bar{d}/B}(x_2, \mu_f) [A_0^S + A_0^V + A_0^{SC}(u \rightarrow ug) \\ & + A_0^{SC}(\bar{d} \rightarrow \bar{d}g)] + \tilde{G}_{u/A}(x_1, \mu_f) G_{\bar{d}/B}(x_2, \mu_f) \\ & + G_{u/A}(x_1, \mu_f) \tilde{G}_{\bar{d}/B}(x_2, \mu_f) + (A \leftrightarrow B) \}. \end{aligned} \quad (26)$$

And the three-body term, $\sigma_{3S_1^{(8)}}^{(3)}$, is written as

$$\sigma_{3S_1^{(8)}}^{(3)} = \sigma_g^{\overline{HC}}(3S_1^{(8)}) + \sigma_q^{\overline{C}}(3S_1^{(8)}). \quad (27)$$

$\sigma_{3P_J^{(8)}}$ also can be divided into two parts: a two-body term $\sigma_{3P_J^{(8)}}^{(2)}$ and a three-body term $\sigma_{3P_J^{(8)}}^{(3)}$. The two-body term, $\sigma_{3P_J^{(8)}}^{(2)}$, is expressed as

$$\begin{aligned} \sigma_{3P_J^{(8)}}^{(2)} = & \int dx_1 dx_2 d\hat{\sigma}_g^S(3P_J^{(8)}) \{ G_{u/A}(x_1, \mu_f) G_{\bar{d}/B}(x_2, \mu_f) \\ & + (A \leftrightarrow B) \}. \end{aligned} \quad (28)$$

And the three-body term, $\sigma_{3P_J^{(8)}}^{(3)}$, is written as

$$\sigma_{3P_J^{(8)}}^{(3)} = \sigma_g^H(3P_J^{(8)}) + \sigma_q(3P_J^{(8)}). \quad (29)$$

Finally, after taking into account the NRQCD NLO corrections to the operator $\langle \mathcal{O}^{J/\psi}[3S_1^{(8)}] \rangle$, the contributions of the $3S_1^{(8)}$ and $3P_J^{(8)}$ states are finite. As for the contribution from $1S_0^{(8)}$ state, it contains no singularity and only involves a three-body term $\sigma_{1S_0^{(8)}}^{(3)}$, which can be expressed as

$$\sigma_{1S_0^{(8)}} = \sigma_g(1S_0^{(8)}) + \sigma_q(1S_0^{(8)}). \quad (30)$$

As a check of the correctness of our calculations, the independence of the cross section part of $\sigma_{3S_1^{(8)}} + \sigma_{1S_0^{(8)}} + \sigma_{3P_J^{(8)}}$, on the two arbitrary cutoffs, δ_s and δ_c , has been numerically verified.

For the $pp \rightarrow J/\psi + W + X$ process at the LHC, we take CTEQ6L1 PDFs with an one-loop running α_s in the LO calculations, and CTEQ6M PDFs with a two-loop α_s in the NLO calculations [33]. For the QCD parameters we take the number of active flavor as $n_f = 3$, and input $\Lambda_{\text{QCD}}^{(3)} = 249$ MeV for the LO and $\Lambda_{\text{QCD}}^{(3)} = 389$ MeV for the NLO calculations [11], respectively. The masses of the external particles and the fine structure constant are taken as $m_W = 80.398$ GeV, $m_c = m_{J/\psi}/2 = 1.5$ GeV and $\alpha = 1/137.036$. The sine squared of the Weinberg angle is expressed as

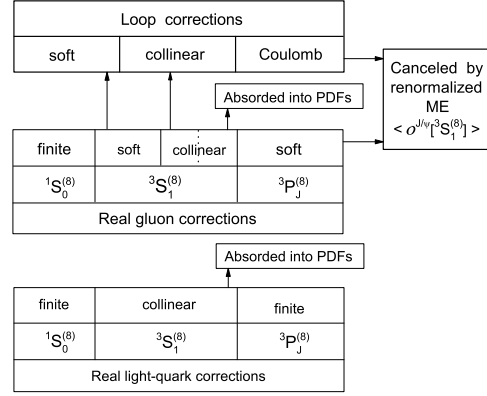


FIG. 2: The IR and Coulomb singularities structure in the NLO QCD calculations for the $pp \rightarrow J/\psi + W^+ + X$ process.

$s_W^2 = 1 - m_W^2/m_Z^2$, where $m_Z = 91.1876$ GeV. The renormalization, factorization and NRQCD scales are chosen as $\mu_r = \mu_f = m_T$ and $\mu_\Lambda = m_c$, respectively, where $m_T = \sqrt{(p_T^{J/\psi})^2 + m_{J/\psi}^2}$ is the J/ψ transverse mass. Since the $\langle \mathcal{O}^{J/\psi}[3P_J^{(8)}] \rangle$ ($J = 0, 1, 2$) LDMEs satisfy the multiplicity relations

$$\langle \mathcal{O}^{J/\psi}[3P_J^{(8)}] \rangle = (2J+1) \langle \mathcal{O}^{J/\psi}[3P_0^{(8)}] \rangle,$$

we adopt the LDME $\langle \mathcal{O}^{J/\psi}[3S_1^{(8)}] \rangle = 2.73 \times 10^{-3} \text{ GeV}^3$ and the linear combination

$$M_r^{J/\psi} = \langle \mathcal{O}^{J/\psi}[1S_0^{(8)}] \rangle + \frac{r}{m_c^2} \langle \mathcal{O}^{J/\psi}[3P_0^{(8)}] \rangle$$

with $M_r^{J/\psi} = 5.72 \times 10^{-3} \text{ GeV}^3$ and $r = 3.54$ as the input parameters, which were fitted to the Tevatron RUN-I data by using the CTEQ4 PDFs and have taken into account the dominant higher-order effects due to the multiple-gluon radiation in the inclusive J/ψ hadroproduction [34]. Then the $\langle \mathcal{O}^{J/\psi}[1S_0^{(8)}] \rangle$ and $\langle \mathcal{O}^{J/\psi}[3P_0^{(8)}] \rangle$ LDMEs are fixed by the democratic choice [35]

$$\langle \mathcal{O}^{J/\psi}[1S_0^{(8)}] \rangle = \frac{r}{m_c^2} \langle \mathcal{O}^{J/\psi}[3P_0^{(8)}] \rangle = \frac{1}{2} M_r^{J/\psi}.$$

In the calculations of the real corrections, the two phase space cutoffs are chosen as $\delta_s = 10^{-3}$ and $\delta_c = \delta_s/50$, and the invariance of the δ_s value running in the range of $10^{-4} - 10^{-2}$ is checked within the error tolerance. Considering the validity of the NRQCD and perturbation method, we restrict our results in the range of $p_T^{J/\psi} > 3$ GeV and $|y_{J/\psi}| < 3$.

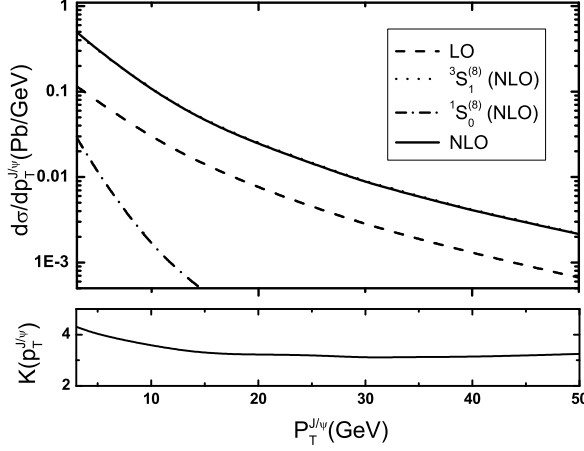


FIG. 3: The LO and NLO QCD corrected distributions of $p_T^{J/\psi}$ for the $pp \rightarrow J/\psi + W^\pm + X$ process, and the contributions of the $c\bar{c}[^1S_0^{(8)}]$ and $c\bar{c}[^3S_1^{(8)}]$ Fock states up to NLO at the LHC.

In Fig.3, we present the LO and NLO QCD corrected distributions of $p_T^{J/\psi}$ for the $pp \rightarrow J/\psi + W^\pm + X$ process at the LHC. For comparison, we also depict the contributions of the $c\bar{c}[^1S_0^{(8)}]$ and $c\bar{c}[^3S_1^{(8)}]$ Fock states in the figure, while the total contribution of the $c\bar{c}[^3P_J^{(8)}]$ ($J = 0, 1, 2$) Fock states is negative and will be drawn in Fig.4. From the Fig.3 we can see that the differential cross section at the LO is significantly enhanced by the QCD corrections. In the range of $3 \text{ GeV} < p_T^{J/\psi} < 50 \text{ GeV}$, the K -factor, defined as $K = \frac{d\sigma^{NLO}}{dp_T^{J/\psi}} / \frac{d\sigma^{LO}}{dp_T^{J/\psi}}$, is in the range of $[3.09, 4.31]$, and reaches its maximum when $p_T^{J/\psi} = 3 \text{ GeV}$. In Fig.4, we present the various contributions of the $c\bar{c}[^3P_J^{(8)}]$ Fock states. The solid, dashed and dash-dotted curves represent the total contribution of the $c\bar{c}[^3P_J^{(8)}]$ Fock states, the real gluon emission correction to the $c\bar{c}[^3P_J^{(8)}] + W$ production and the real light-quark emission correction to the $c\bar{c}[^3P_J^{(8)}] + W$ production, respectively. In Figs.3 and 4, we can see that there exists a compensation between the contributions of the S and P states. The contributions of the $c\bar{c}[^1S_0^{(8)}]$, $c\bar{c}[^3S_1^{(8)}]$ Fock states and the real light-quark emission correction to the $c\bar{c}[^3P_J^{(8)}] + W$ production are always positive, while the real gluon emission correction to the $c\bar{c}[^3P_J^{(8)}] + W$ production is negative.

In above calculations, we mainly consider the direct production of J/ψ mesons up to the NLO. But

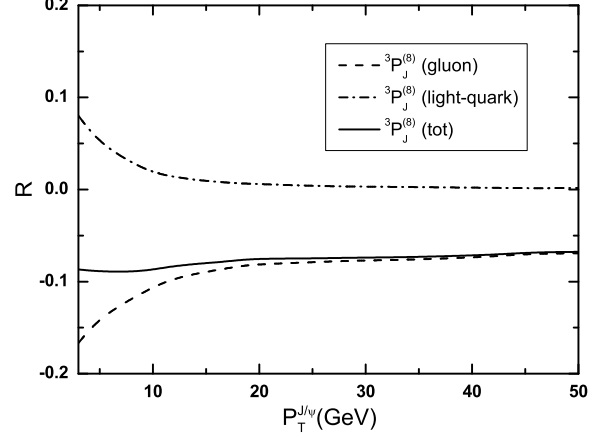


FIG. 4: The ratio R versus $p_T^{J/\psi}$ with the definition of $R \equiv \frac{d\sigma^{3P_J^{(8)}}}{dp_T^{J/\psi}} / \frac{d\sigma^{LO}}{dp_T^{J/\psi}}$.

the J/ψ also can be produced indirectly via radiative or hadronic decays of heavier charmonia, such as χ_{cJ} and ψ' mesons. The respective decay branching fractions are $B(\chi_{c0} \rightarrow J/\psi + \gamma) = (1.28 \pm 0.11)\%$, $B(\chi_{c1} \rightarrow J/\psi + \gamma) = (36.0 \pm 1.9)\%$, $B(\chi_{c2} \rightarrow J/\psi + \gamma) = (20.0 \pm 1.0)\%$ and $B(\psi' \rightarrow J/\psi + X) = (57.4 \pm 0.9)\%$ [36]. The cross sections for these four indirect production channels can be obtained approximately by multiplying the direct-production cross sections for the respective intermediate charmonia by their decay branching fractions. At the LO, only the $c\bar{c}[^3S_1^{(8)}]$ color-octet contributes to the productions of the charmonia associated with a W boson at the LHC. With the multiplicity relations of LDMEs $\langle \mathcal{O}^{\chi_{cJ}}[^3S_1^{(8)}] \rangle$, $\langle \mathcal{O}^{\chi_{cJ}}[^3S_1^{(8)}] \rangle = (2J+1) \langle \mathcal{O}^{\chi_{c0}}[^3S_1^{(8)}] \rangle$, the cross sections for the productions of the charmonia associated with W can be expressed as

$$d\hat{\sigma}(pp \rightarrow H + W) = d\hat{\sigma}_0 \frac{\langle \mathcal{O}^H[^3S_1^{(8)}] \rangle}{\langle \mathcal{O}^{J/\psi}[^3S_1^{(8)}] \rangle}, \quad (31)$$

where H represents the intermediate charmonia ψ' or χ_{cJ} . In numerical calculations, we adopt the LDMEs $\langle \mathcal{O}^{\chi_{c0}}[^3S_1^{(8)}] \rangle = (6.81 \pm 1.75) \times 10^{-4} \text{ GeV}^3$ [34] and $\langle \mathcal{O}^{\psi'}[^3S_1^{(8)}] \rangle = (2.0 \pm 0.2) \times 10^{-3} \text{ GeV}^3$ [37]. We find that the cross section for the indirect J/ψ production is almost the same as the LO cross section for the direct J/ψ production, $\sigma^{\text{indirect}} = 0.94 \times \sigma^{(0)}$. The complete indirect J/ψ production in association with a W

gauge boson at the NLO will be calculated in our further work.

In this paper we investigate the NLO QCD corrections to the $J/\psi + W$ production at the LHC, and present the numerical results of the differential cross section of the $p_T^{J/\psi}$ and the contributions of the different Fock states for the $pp \rightarrow J/\psi + W + X$ process up to the QCD NLO. We find that the differential cross section at the LO is significantly enhanced by the QCD corrections. The numerical results show that there exists a negative real gluon emission correction to the $c\bar{c}[^3P_J^{(8)}] + W$ production. The LO differential cross section for the process $pp \rightarrow J/\psi + W^\pm + X$ in the low $p_T^{J/\psi}$ region is heavily enhanced, and the NLO QCD corrected differential cross section can reach 0.49 pb in the vicinity of $p_T^{J/\psi} \sim 3 \text{ GeV}$. Although the J/ψ events are difficult to be accepted at low p_T region, we can find that the cross section for $J/\psi + W$ direct production at the NLO is about 0.81 pb with $p_T^{J/\psi} > 10 \text{ GeV}$. To obtain the cross section for the process $pp \rightarrow J/\psi + W + X$ with the pure leptonic decays, we multiply the cross section for the direct production by the branching fractions 12% for $J/\psi \rightarrow l^+ l^-$ and 22% for $W \rightarrow l\nu$. Given the integrated luminosity of 300 fb^{-1} at the LHC, we could obtain about 6400 events. If we include the indirect contribution of the radiative or hadronic decays of χ_{cJ} and ψ' mesons to J/ψ , more events could be detected. Even taking into account the detector acceptance and efficiency, there are still enough $J/\psi + W$ events which can be detected. We conclude that the LHC has the potential to detect the $J/\psi + W$ production. If the $J/\psi + W$ production is really detected, it would be a solid basis for testing the colour-octet mechanism of the NRQCD.

Acknowledgments: This work was supported in part by the National Natural Science Foundation of China(No.10875112, No.11075150, No.11005101), the Specialized Research Fund for the Doctoral Program of Higher Education(No.20093402110030), and the 211 Project of Anhui University.

-
- [1] G.T. Bodwin, E. Braaten, and G.P. Lepage, Phys. Rev. D **51**, 1125 (1995); **55**, 5853(E) (1997).
 - [2] G.P. Lepage, L. Magnea, C. Nakhleh, U. Magnea, and K. Hornbostel, Phys. Rev. D **46**, 4052 (1992).
 - [3] H.W. Huang and K.T. Chao, Phys. Rev. D **54**, 3065 (1996); **56**, 7472(E) (1997); **55**, 244 (1997); **54**, 6850 (1996); **56**, 1821(E) (1997).
 - [4] A. Petrelli, M. Cacciari, M. Greco, F. Maltoni, and M.L. Mangano, Nucl. Phys. B **514**, 245 (1998).
 - [5] Z.G. He, Y. Fan, and K.T. Chao, Phys. Rev. Lett. **101**, 112001 (2008).
 - [6] Y. Fan, Z.G. He, Y.Q. Ma, and K.T. Chao, Phys. Rev. D **80**, 014001 (2009).
 - [7] E. Braaten and S. Fleming, Phys. Rev. Lett. **74**, 3327 (1995).
 - [8] J. Abdallah *et al.* (DELPHI Collaboration), Phys. Lett. B **76**, 565 (2003).
 - [9] M. Klasen, B.A. Kniehl, L.N. Mihaila, and M. Steinhauser, Phys. Rev. Lett. **89**, 032001 (2002).
 - [10] C. Adloff *et al.* (H1 Collaboration), Eur. Phys. J. C **25**, 25 (2002); M. Steder, on behalf of the H1 Collaboration, Report No. H1prelim-07-172.
 - [11] M. Butenschoen and B.A. Kniehl, Phys. Rev. Lett. **104**, 072001 (2010).
 - [12] K. Abe *et al.* (BELLE Collaboration), Phys. Rev. Lett. **89**, 142001 (2002); B. Aubert *et al.* (BABAR Collaboration), Phys. Rev. D **72**, 031101 (2005); P. Pakhlov *et al.* (Belle Collaboration), Phys. Rev. D **79**, 071101 (2009).
 - [13] E. Braaten and J. Lee, Phys. Rev. D **67**, 054007 (2003); **72**, 099901(E) (2005); K.Y. Liu, Z.G. He, and K.T. Chao, Phys. Lett. B **557**, 45 (2003); Phys. Rev. D **77**, 014002 (2008); K. Hagiwara, E. Kou, and C.F. Qiao, Phys. Lett. B **570**, 39 (2003).
 - [14] Y.J. Zhang, Y.J. Gao, and K.T. Chao, Phys. Rev. Lett. **96**, 092001 (2006); Y.J. Zhang and K.T. Chao, Phys. Rev. Lett. **98**, 092003 (2007); B. Gong and J.X. Wang, Phys. Rev. D **77**, 054028 (2008); **80**, 054015 (2009); Phys. Rev. Lett. **100**, 181803 (2008); Y.J. Zhang, Y.Q. Ma, and K.T. Chao, Phys. Rev. D **78**, 054006 (2008).
 - [15] G.T. Bodwin, D. Kang, and J. Lee, Phys. Rev. D **74**, 014014 (2006); **74**, 114028 (2006); Z.G. He, Y. Fan, and K.T. Chao, Phys. Rev. D **75**, 074011 (2007).
 - [16] Y.Q. Ma, Y.J. Zhang, and K.T. Chao, Phys. Rev. Lett. **102**, 162002 (2009); B. Gong and J.X. Wang, Phys. Rev. Lett. **102**, 162003 (2009).
 - [17] E. Braaten, B. A. Kniehl, and J. Lee, Phys. Rev. D **62**, 094005 (2000); B. A. Kniehl and J. Lee, Phys. Rev. D **62**, 114027 (2000).
 - [18] P. Artoisenet, J. Campbell, F. Maltoni, and F. Tramontano, Phys. Rev. Lett. **102**, 142001 (2009).
 - [19] B.A. Kniehl, C.P. Palisoc, and L. Zwierner, Phys. Rev. D **66**, 114002 (2002). V. Barger, S. Fleming, R.J.N. Phillips, Phys. Lett. B **371**, 111 (1996).
 - [20] M. Kramer, Nucl. Phys. B **459**, 3 (1996); R. Li and J.X. Wang, Phys. Lett. B **672**, 51 (2009).
 - [21] J. Campbell, F. Maltoni, and F. Tramontano, Phys. Rev. Lett. **98**, 252002 (2007); B. Gong and J.X. Wang, Phys. Rev. Lett. **100**, 232001 (2008); Phys. Rev. D **78**, 074011 (2008); B. Gong, X.Q. Li, and J.X. Wang Phys. Lett. B **673**, 197 (2009); P. Artoisenet, J. Campbell, J. P. Lansberg, F. Maltoni, and F. Tramontano, Phys. Rev. Lett. **101**, 152001 (2008).
 - [22] G. 't Hooft and M. Veltman, Nucl. Phys. B **153**, 365 (1979).
 - [23] A. Denner, U. Nierste, and R. Scharf, Nucl. Phys. B **367**, 637 (1991).

- [24] A. Denner and S. Dittmaier, Nucl. Phys. B **658**, 175 (2003).
- [25] M. Kramer, Nucl. Phys. B **459**, 3 (1996).
- [26] R.K. Ellis and G. Zanderighi, JHEP **0802**, 002 (2008).
- [27] B.W. Harris and J.F. Owens, Phys. Rev. D **65**, 094032 (2002).
- [28] W.Beenakker, H.Kuijf, W.L.van Neerven, and J.Smith, Phys. Rev.D **40**,54 (1989);
J.Smith, D.Thomas,and W.L.van Neerven, Z.Phys. C **44**,267(1989).
- [29] W.L.van Neerven, Nucl. Phys. B **268**(1986)453.
- [30] B.W.Harris and J.Smith, Nucl. Phys. B **452** (1995) 109.
- [31] G. Altarelli and G. Parisi, Nucl. Phys. B **126** 298 (1997).
- [32] B.W. Harris, J.F. Owens, Phys. Rev. D **65**(2002) 094032.
- [33] J. Pumplin, D.R. Stump, J. Huston, H.L. Lai, P. Nadolsky, and W.K. Tung, JHEP **0207**, 012 (2002).
- [34] B. A. Kniehl and G. Kramer, Eur. Phys. J. C **6**, 493 (1999).
- [35] M. Klasen, B. A. Kniehl, L. N. Mihaila, and M. Steinhauser, Nucl. Phys. B **713**, 487 (2005); Phys. Rev. D **71**, 014016 (2005).
- [36] Particle Data Group, C.Amsler *et al.*, Phys. Lett. B **667**, 1 (2008).
- [37] B. A. Kniehl and C. P. Palisoc, Eur. Phys. J. C **48**, 451 (2006).